

Exact non-Hookean scaling of cylindrically bent elastic sheets and the large-amplitude pendulum

Vyacheslavas Kashcheyevs*

Faculty of Physics and Mathematics, University of Latvia, Zellu street 8, Riga LV-1002, Latvia

A sheet of elastic foil rolled into a cylinder and deformed between two parallel plates acts as a non-Hookean spring if deformed normally to the axis. For large deformations the elastic force shows an interesting inverse squares dependence on the interplate distance [Šiber and Buljan, arXiv:1007.4699 (2010)]. The phenomenon has been used as a basis for an experimental problem at the 41st International Physics Olympiad. We show that the corresponding variational problem for the equilibrium energy of the deformed cylinder is equivalent to a minimum action description of a simple gravitational pendulum with an amplitude of 90° . We use this analogy to show that the power-law of the force is exact for distances less than a critical value. An analytical solution for the elastic force is found and confirmed by measurements over a range of deformations covering both linear and non-Hookean behavior.

I. INTRODUCTION

In a recent study,¹ Šiber and Buljan analyze the following simple yet pedagogically rich problem from the theory of elasticity. A thin flat elastic sheet (e.g., a piece of plastic foil) is rolled into a cylinder (radius b_0) and placed between two impenetrable plates which are parallel to each other and to the axis of the cylinder, see Fig. 1. The distance $2b$ between the plates is fixed externally. For $b < b_0$ the foil acts as a spring exerting a force of magnitude $F(b)$ on each of the plates. An interesting property for this kind of spring is the non-Hookean power-law scaling of the elastic force,¹ $F \propto b^{-2}$, which holds (as we show here, *exactly*) for $b < b_c \simeq 0.7b_0$. Measuring $F(b)$ in this universal scaling regime has been proposed¹ as a method to determine bending rigidity for such objects as plastic foils, electrical connectors, biological membranes and microtubules, possibly nanotubes and monolayer materials (e.g., graphene) etc. A lab problem based on measuring of $F(b)$ for standard plastic transparency films has been recently given to world's top secondary school physics students at the 41st International Physics Olympiad (Zagreb, Croatia, 2010).

The corresponding mathematical problem of constrained minimization of the foil's elastic energy may seem difficult and hardly illuminating. Existing solution¹ is based on analytical approximations and numerical finite element optimization while a textbook approach² relies on force equilibrium conditions for strongly bent elastic rods that are rarely covered in standard physics curricula.

In this paper we formulate and solve the variational problem using tangential angle parametrization of the profile shape. This reveals equivalence to another conceptually rich physics system — the large-amplitude pendulum: elastic energy of the foil maps onto kinetic energy of the pendulum while the fixed inter-plate distance translates into the cosine-shape potential energy. Simple mechanical considerations allow us to deduce the exact inverse squares law for the elastic force at $b < b_c$. Using the standard solution for the large-amplitude pendulum

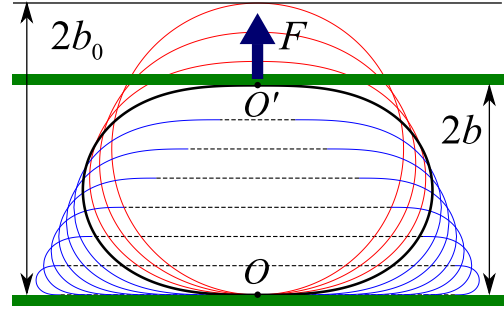


FIG. 1. A thin-walled elastic tube deformed between two parallel plates. The thick black contour line marks the profile at the critical value of $b_c/b_0 = 0.717770$, thinner lines above and below correspond to different b/b_0 between 0 and 1.

in terms of elliptic functions, we find (a) the exact values for b_c and related constants; (b) a single transcendental equation that determines $F(b)$ for $b > b_c$; and (c) compact analytic form of the universal profile. Finally, the deduced functional dependence $F(b)$ is compared to measurements on a plastic film in the table-top setup used in Ref. 1. This shows feasibility of a quantitative demonstration of both the universal non-Hookean law for $b < b_c$ and the usual linear regime for $b \rightarrow b_0$.

II. FORMULATION OF THE PROBLEM

Specific property of the deformation geometry in this problem is “cylindricity”: the Gaussian curvature vanishes at every point. This eliminates non-uniform stretching/compression (§14 of Ref. 2) and leaves only the bending contribution to the total elastic energy W_{el} for thin sheets (thickness $d \ll b_0$). The problem is essentially one-dimensional and the energy functional (1) is the same as for an elastic filament (Kirchhoff rod, see §18 of Ref. 2):

$$W_{el} = \frac{\kappa h}{2} \int \mathcal{K}^2 ds. \quad (1)$$

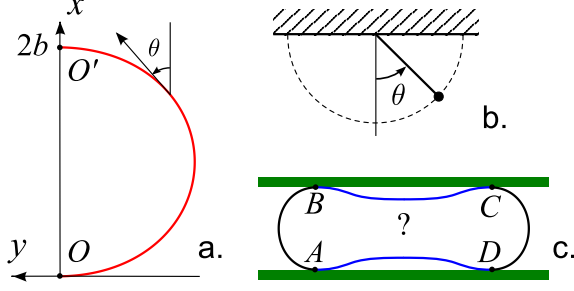


FIG. 2. (a) Coordinate system for profile energy calculation. (b) Equivalent pendulum problem with 90° maximal deviation. (c) A possible four contact-point profile.

(This effects of gravity are ignored.) Here $\kappa = (1 - \nu^2)^{-1}Ed^3/12$ is the bending rigidity, E is the bulk Young modulus of the foil material, ν is the Poisson ratio, h is the length of the cylinder in the non-deformed direction (i.e. parallel to the axis), and \mathcal{K} is the planar curvature of the deformation profile in the plane normal to the axis (x - y plane). The shape of the profile is described using natural parametrization³ $\{x(s), y(s)\}$ in the coordinate system defined in Fig. 2a with origin at point O ; s is the arc length measured counter-clockwise from O . Integration in (1) is performed along the entire profile, and the absence of stretching⁴ implies that $\int ds = 2\pi b_0$ regardless of b . The constraint imposed by the plates is expressed by requesting that the vertical coordinate of point O' is $2b$ (see Fig. 2a),

$$x(s=\pi b_0) = 2b. \quad (2)$$

In the following we find the minimum of W_{el} subject to the constraint (2) and taking into account impenetrability of the plates. The elastic force is then obtained from $F(b) = -dW_{\text{el}}/d(2b)$.

III. ANALYTIC SOLUTION

A. Lagrangian formulation and analogy to the pendulum

An intrinsic quantity characterizing the shape of a planar curve is its tangential angle $\theta(s)$ defined as $\{\dot{x}, \dot{y}\} = \{\cos \theta, \sin \theta\}$ (dot denotes derivative with respect to s). Particular advantage of employing $\theta(s)$ for the present problem is that the (signed) curvature equals³ to simply $\mathcal{K} = \dot{\theta}$. Integrating $\dot{x} = \cos \theta$ over the right half of the profile between the contact points O and O' gives the expression of the constraint (2) in integral form:

$$\int_0^{\pi b_0} \cos \theta(s) ds = 2b = \frac{2b}{\pi b_0} \int_0^{\pi b_0} ds. \quad (3)$$

At the points of contact between the foil and the plates, the tangent to the profile must be parallel to the y -axis,

hence the boundary conditions for $\theta(s)$,

$$\theta(s=0) = -\pi/2, \quad \theta(s=\pi b_0) = +\pi/2. \quad (4)$$

A standard way of turning a constrained optimization problem to an unconstrained one is the use of Lagrange multipliers. In our problem both the target function W_{el} and the constraint (3) are expressed as integrals (functionals) of the unknown function $\theta(s)$. Denoting the Lagrange multiplier for Eq. (3) by ω_0^2 (for reasons that will become clear shortly) and using left-right symmetry in Eq. (1), the variational problem becomes that of unconstrained minimization with respect to a function $\theta(s)$ and a number ω_0^2 of the following functional

$$\widetilde{W} = \frac{1}{2} \frac{W_{\text{el}}}{\kappa h} = \int_0^{\pi b_0} \mathcal{L}[\theta(s), \dot{\theta}(s), \omega_0^2] ds \quad (5)$$

where

$$\mathcal{L} = \frac{1}{2} \dot{\theta}^2 + \omega_0^2 \cos \theta - \omega_0^2 \frac{2b}{\pi b_0}. \quad (6)$$

Now the analogy to the pendulum problem has become manifest. Viewing \widetilde{W} as dynamical action and s as time, one recognizes in Eq. (6) the Lagrange function of a rigid pendulum in uniform gravitational field with the angular frequency of *small* oscillations equal to ω_0 (see schematic drawing in Fig. 2b). In the pendulum problem, θ is the angle of deviation from the stable equilibrium which must satisfy the Newton's equation (Euler-Lagrange equation of the variational problem)⁵,

$$\ddot{\theta} + \omega_0^2 \sin \theta = 0. \quad (7)$$

In standard mechanics problems ω_0 is usually given, and the fulfillment of the boundary conditions (4) is ensured by choosing the appropriate initial velocity $\dot{\theta}(0) \equiv \mathcal{K}_0$ which is a function of ω_0 . In our case, both ω_0 and \mathcal{K}_0 are not known *a priori* and must be determined by satisfying both the boundary conditions (4) and the constraint (3). The optimal value of ω_0^2 is proportional *the elastic force itself* since, after “integrating out” the pendulum degree of freedom [i.e. substituting $\theta(s)$ in the Lagrange function with the solution to the equation of motion (7)], $\widetilde{W}(\omega_0, b)$ satisfies $\partial \widetilde{W} / \partial \omega_0 = 0$ and thus

$$F = -\kappa h \frac{d\widetilde{W}(\omega_0, b)}{db} = -\kappa h \frac{\partial \widetilde{W}}{\partial b} = 2\kappa h \omega_0^2. \quad (8)$$

We shall use this neat property of Lagrange multipliers for the calculation of $F(b)$.

Before tackling the problem of finding \mathcal{K}_0 and ω_0 (which is mostly mathematical), we develop physical arguments for the universal scaling behavior which constitute, in author's opinion, the most important message of this article.

B. Universal regime, $b \leq b_c$

Qualitatively, $\mathcal{K}_0(b)$ starts from the value of $\mathcal{K}_0(b_0) = 1/b_0$ and decreases as b is decreased. At a certain critical (in the sense of separating two qualitatively different behaviors) $b = b_c$ the contact curvature vanishes, $\mathcal{K}_0(b_c) = 0$. The corresponding pendulum problem becomes that of free oscillations with amplitude $\pi/2$ and frequency $\omega_0(b_c) = \omega_c$ (“critical pendulum”). Period of these oscillations is well-known⁶ [also derived below as a special case of Eq. (16)], $T_0 = 4K(1/2)/\omega_c$, where K is complete elliptic integral of the first kind. Since according to Eq. (4) it must be equal to $T_0 = 2\pi b_0$, we get

$$\omega_c = (\zeta_0 b_0)^{-1} \text{ with } \zeta_0 \equiv \frac{\Gamma^2(3/4)}{\sqrt{\pi}} = 0.847213\dots \quad (9)$$

When b is decreased further below b_c , an extra condition not accounted for by the Lagrangian formulation (6) becomes relevant: the plates do not allow the foil to bend outwards, thus \mathcal{K}_0 remains zero also for $b < b_c$. In order to accommodate the imposed small values of b without violating the rigid plates, a finite part of the foil in the vicinity of $s = 0$ and $s = \pi b_0$ must remain flat, $\mathcal{K}(s) = 0$ (these parts are marked by horizontal dashed lines in the profiles shown in Fig. 1). Concurrently, the sections of the profile that do bend obey Newton’s equation (7), although with some $\omega_0(b) > \omega_c$. Assuming continuity in $\mathcal{K}(s)$, we conclude that the deformed part of the profile for $b < b_c$ must start with $\mathcal{K}_0 = 0$ (same as for $b = b_c$) but cover a length shorter than the full length $2\pi b_0$ of the foil cross-section. This shortening of the deformed part can only be accommodated by a faster pendulum since the frequency $\omega_0(b)$ of the latter remains the only adjustable (i.e. b -dependent) parameter in the problem for $b < b_c$. (The other parameter, \mathcal{K}_0 , is pinned to zero by the presence of a finite flat part.) But, according to Eq. (7), changing ω_0 results in a *uniform* rescaling of the arc length parameter s , therefore the bent parts of the profile at $b < b_c$ (marked by curved lines between the plates in Fig. 1) must be *geometrically similar* to the corresponding halves of the critical profile at $b = b_c$ (marked with a thick contour in Fig. 1).

Having established that the *critical* profile shape is also *universal* (in the sense of being applicable to any $b < b_c$), we can determine the scaling law for the force using simple dimensional considerations. Scaling of b and b_0 with b/b_0 fixed does not change the overall shape of the profile — the tangential angle θ remains the same function of s/b_0 . Therefore the elastic energy (1) can be written as¹ $W_{\text{el}}(b) = \kappa h \mathcal{U}(b/b_0)/b_0$ where \mathcal{U} is a dimensionless function of b/b_0 . For $b < b_c$ the flat parts of the profile do not contribute to the energy. The curved parts are similar to the critical profile but b/b_c times smaller, thus their energy must have a fixed $\mathcal{U}(b/b_0) \rightarrow \mathcal{U}(b_c/b_0)$ and rescaled $b_0 \rightarrow b_0 b/b_c$. This argument proves exact scaling for the energy, $W_{\text{el}} \propto b^{-1}$, and, consequently, the force, $F \propto b^{-2}$ for $b < b_c$. The prefactor in the scaling

law can be described as follows:

$$F(b) = F_c \frac{b_c^2}{b^2} = 2\kappa h \frac{(b_c/b_0)^2}{\zeta_0^2} b^{-2} \text{ for } b < b_c. \quad (10)$$

where $F_c \equiv F(b = b_c)$ and Eqs. (8) and (9) have been used. The phenomenological “stadium profile” model, considered as a variational *ansatz* in Ref. 1, assumes circle as a universal profile and predicts $F(b) = (\pi/2)\kappa h/b^{-2}$, similar to Eq. (10). The exact critical shape is, however, more efficient than a circle in minimizing the bending energy. We can calculate the numerical prefactor in Eq. (10) exactly by determining b_c . To this end, we proceed to the integration of the pendulum’s equation of motion.

The first integral of Newton’s equation is the energy conservation law, $\dot{\theta}^2/2 - \omega_0^2 \cos \theta = \text{const.}$ Taking into account $\cos \theta(s=0) = 0$ gives

$$\frac{1}{2}\dot{\theta}^2 = \frac{1}{2}\mathcal{K}_0^2 + \omega_0^2 \cos \theta. \quad (11)$$

Integrating both sides of Eq. (11) with respect to s and with respect to θ , then using Eq. (3) gives

$$\widetilde{W} = \frac{1}{2} \int_0^{\pi b_0} \dot{\theta}^2 ds = \frac{\pi b_0 \mathcal{K}_0^2}{2} + 2\omega_0^2 b, \quad (12)$$

$$\widetilde{W} = \frac{1}{2} \int_{-\pi/2}^{+\pi/2} \dot{\theta} d\theta = \omega_0 I_0(\mathcal{K}_0/\omega_0), \quad (13)$$

where

$$I_n(\alpha) \equiv (1/2) \int_{-\pi/2}^{+\pi/2} (\alpha^2 + 2 \cos \theta)^{1/2-n} d\theta. \quad (14)$$

Now b_c can be determined from Eqs. (12) and (13): substituting b_c , ω_c , and 0 for b , ω_0 , and \mathcal{K}_0 respectively, and using an identity $\zeta_0 = I_0(0)/2$, one gets

$$b_c = I_0(0)/(2\omega_c) = \zeta_0^2 b_0 = 0.717770\dots \times b_0. \quad (15)$$

The results (10) and (15) confirm phenomenological Eq. (17) of Ref. 1 (with numerical factor 0.912 there corrected to $4\zeta_0^2/\pi = 0.91389$).

C. Small deformations, $b_0 > b > b_c$

In this regime $\mathcal{K}_0 > 0$ and the relation between the period and the boundary conditions becomes more complicated. Expressing $\omega_0 ds$ via $d\theta$ from Eq. (11) and integrating over from $s = 0$ to $s = \pi b_0$, we obtain the required additional equation,

$$\pi b_0 \omega_0 = 2I_1(\mathcal{K}_0/\omega_0). \quad (16)$$

This equation will provide the answer for the force, thanks to Eq. (8). The remaining unknown is the parameter $\alpha \equiv \mathcal{K}_0/\omega_0$, for which a single transcendental

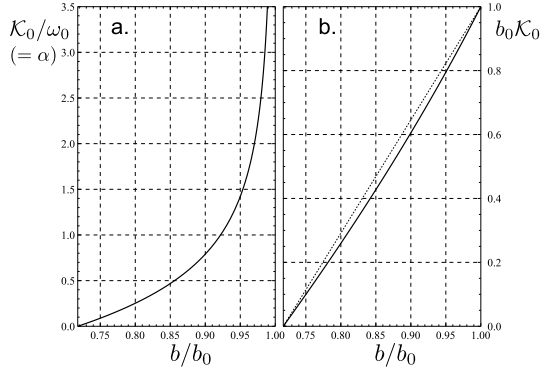


FIG. 3. (a) Graphical solution of Eq. (17). (b) The curvature at the contact point \mathcal{K}_0 as a function of b/b_0 . The dashed straight line $(b - b_c)/(b_0 - b_c)$ is plotted for visual guidance.

equation is easily derived by combining Eqs. (12), (13), and (16),

$$\frac{b}{b_0} = \frac{\pi}{4} \left(\frac{I_0(\alpha)}{I_1(\alpha)} - \alpha^2 \right). \quad (17)$$

The functions I_n , defined as integrals and appearing in Eqs. (13), (16) and (17), can be reduced to standard elliptic integrals,⁷ $I_0(\alpha) = (4/k)\mathcal{E}(\pi/4, k^2)$ and $I_1(\alpha) = k\mathcal{F}(\pi/4, k^2)$, where \mathcal{E} and \mathcal{F} are incomplete elliptic integrals of the first and the second kind, respectively, and $k \equiv 2/\sqrt{2 + \alpha^2}$ is the elliptic modulus. $I_1(0) = K(1/2) = \pi/(2\zeta_0)$ in consistence with Eq. (9). We were unable, however, to solve the transcendental Eq. (17) analytically and present a graphical solution instead, see Fig. 3a.

As b/b_0 changes from b_c/b_0 to 1, the only root of Eq. (17) goes from 0 to ∞ . Divergence of $\alpha = \mathcal{K}_0/\omega_0$ as $b \rightarrow b_0$ is consistent with $\omega_0^2 \propto F \rightarrow 0$. The curvature at the contact point $\mathcal{K}_0 = \alpha\omega_0$ is plotted separately in Fig. 3b; \mathcal{K}_0 decreases from $1/b_0$ to 0 as b goes from b_0 to b_c , in accordance with our previous qualitative discussion.

Summing up the solution for $b > b_c$, the exact elastic energy and the force are

$$W_{\text{el}} = \frac{4\kappa h}{\pi b_0} I_0(\alpha) I_1(\alpha), \quad (18)$$

$$F = \frac{2\kappa h}{b_0^2} \left(\frac{2I_1(\alpha)}{\pi} \right)^2, \quad (19)$$

where $\alpha(b/b_0)$ is the root of Eq. (17), see Fig. 3a.

D. Stability of the universal solution and bending-induced tension

After formulating an explicit solution for $b > b_c$, Eq. (18), we can justify the universal scaling for $b < b_c$ more rigorously. It has been suggested¹ that at $b \lesssim 0.3b_0$

profiles with a slight curvature in the horizontal part may provide a better solution than a “stadium” with completely flat segments. Such a four-contact-point alternative solution is sketched in Fig. 2c (the concave segments BC and AD are exaggerated). The following argument shows, however, that any four-contact-point profile will have larger bending energy than the optimal profile with straight BC and AD .

Let us fix the positions of the contact points on the profile, e.g., by gluing the foil to the plates at A , B , C , and D . The curvature \mathcal{K}_A must be the same at all of these four points due to symmetry; furthermore, \mathcal{K}_A is evidently positive. Thus the strongly curved parts AB and CD must conform to our solution for $\mathcal{K}_0 = \mathcal{K}_A > 0$ with a smaller b_0 , adjusted to their respective shorter lengths. Consider now increasing slightly the lengths of AB and CD while making BC and AD shorter so that the total circumference of the profile remains the same. In this new configuration the energy of the segments BC and AD will evidently be reduced by shortening. However, the corresponding lengthening of the segments AB and CD shall *also reduce* their energy: for fixed b , longer (higher b_0) two-point profiles have *lower* minimal total energy. This can be shown explicitly using Eqs. (8), (16), (18) and (19):

$$F_T \equiv \frac{dW_{\text{el}}}{d(2\pi b_0)} \Big|_{b=\text{const}} = -\frac{\kappa h}{2} \mathcal{K}_0^2 \leq 0. \quad (20)$$

Thus one can always lower the bending energy of a four-point profile like the one shown in Fig. 2c down to the point where BC and AD become completely flat and can no longer be shortened. This minimal energy limit is precisely our zero-contact-curvature universal stadium profile.

It is instructive to note that F_T/h is, by definition, the surface tension energy of the deformed foil. Uniform tension may be induced in a cylindrically deformed sheet by bending even if the stretching deformation is negligible.² The value (20) for F_T and its independence of s can be confirmed using a formal method of local Lagrange multipliers⁸ which takes local tension into account explicitly.

Recalling that our sheet is assumed to be made of uniform elastic material with bulk Young modulus E , we can now estimate the neglected stretching deformation. Bending-induced negative surface tension is balanced by uniform linear stretching. By using Hooke’s law, we can express the increment in the profile circumference $2\pi\Delta b_0$ due to stretching as $\Delta b_0 = b_0 F_T/(Edh)$. The corresponding contribution of stretching $\Delta W_{\text{stretch}} \sim Ehd^5/b_0^3$ to the total energy $W \sim Ehd^3/b_0$ is negligible if $d^2 \ll b_0^2$, thus confirming our approximation of an unstretchable foil. The universal profile is tension free, $F_T(b \leq b_c) = 0$.

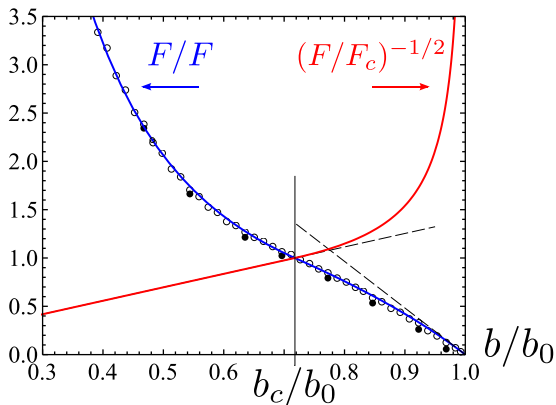


FIG. 4. Elastic force F as a function of the half-height b , scaled by the critical force F_c and the undeformed cylinder radius b_0 , in linear and inverse square root representations. Circles: experimental data scaled by a single fitting parameter, F_c . The spring was first gradually loaded (\circ) up to $b_{\min} = 0.4b_0$ and then unloaded (\bullet).

E. Critical shape

Before discussing our final results for the force, Eqs. (10) and (19), we briefly comment on the shape of the critical profile. Using the explicit solution of the pendulum problem [obtained, e.g., by integrating Eq. (11), see Ref. 6 for a pedagogical presentation], and using properties of the elliptic functions,⁷ the shape of the profile at $b = b_c$, in the units corresponding to $b_0 = 1/(\zeta_0\sqrt{2})$, is given parametrically for $\theta \in [-\pi/2, \pi/2]$ by

$$\begin{cases} x(\theta) &= \zeta_0/\sqrt{2} + \mathcal{E}(\theta/2, \sqrt{2}) , \\ y(\theta) &= \pm\sqrt{\cos\theta} , \end{cases} \quad (21)$$

with the arc length $s(\theta) = \pi b_0/2 + \mathcal{F}(\theta/2, \sqrt{2})$. This shape is shown in Fig. 1 by the thick contour touching the plates. Profile shapes for $b > b_c$ are obtained by integrating Eq. (7) numerically with the initial condition obtained from Eqs. (16) and (17) and shown by thin lines reaching above the upper plate in Fig. 1.

IV. DISCUSSION AND COMPARISON TO EXPERIMENT

The final results for the force are shown in Fig. 4. We use $F_c = 2\kappa h/(\zeta_0 b_0)^2$ to scale the force into a dimensionless form, $F(b)/F_c$, which is a single universal function of b/b_0 . This function is shown by continuous lines in Fig. 4 both in terms of $F(b)/F_c$ and $(F(b)/F_c)^{-1/2}$ to reveal the region of power-law scaling. The point at $b = b_c$ is an inflection point of $F(b)$ (with a jump in the third derivative).

It is instructive to verify that the rolled foil behaves as a Hookean spring when close to cylindrical shape (i.e. as $b \rightarrow b_0$). Using the definition of $I_n(\alpha)$ to get the large α expansion, we obtain α from Eq. (17), $b_0 - b \sim (\pi/4 - 2/\pi)\alpha^{-2}b_0$, and $F(b)$ from Eq. (19) as follows

$$F(b) = \frac{2\kappa h}{b_0^2} \frac{b_0 - b}{b_0} \frac{4\pi}{\pi^2 - 8} \text{ for } b \rightarrow b_0. \quad (22)$$

This linear behavior is marked by a dashed line in lower right corner of Fig. 4.

Measurements of $F(b)$ have been performed using the setup and one of the samples (blue plastic binding covers, Set 1) described in Ref. 1. The results are shown in Fig. 4 by circles on a *linear scale* (cf. the logarithmic scale used in Fig. 5 of Ref. 1). The spring was gradually loaded from $b = b_0$ down to $b_{\min} = 0.4b_0$ (open circles) and then unloaded back by increasing b up to zero force (filled circles). Note the hysteresis due to inelastic deformations. The corresponding energy losses (hysteresis loop area) are 4% of $W_{\text{el}}(b_{\min})$. The critical force $F_c = 116$ N with relative error of 3% (estimated from the residuals between the open data points and the analytical fit) corresponds to the bending rigidity of $\kappa = (1.48 \pm 0.04)$ mJ in reasonable agreement with Ref. 1.

ACKNOWLEDGMENTS

The author is thankful to Paul Stanley and Eli Raz for inspiring discussions of the problem.

* E-mail: slava@latnet.lv

¹ A. Šiber and H. Buljan, “Theoretical and experimental analysis of a thin elastic cylindrical tube acting as a non-Hookean spring,” arXiv:1007.4699v1.

² L. Landau and E. Lifshitz, *Theory of Elasticity*, 3rd ed. (Pergamon Press, London, 1986),

³ D. J. Struik, *Lectures on Classical Differential Geometry*, 2nd ed. (Dover, New York, 1988),

⁴ The accuracy of the unstretchability assumption will be estimated *a posteriori*.

⁵ For an alternative way to derive Eq. (7), see Ref. 2, Sec. 19, Problem 1.

⁶ A. Beléndez, C. Pascual, D. Méndez, T. Beléndez, and C. Neipp, “Exact solution for the nonlinear pendulum,” *Revista Brasileira de Ensino de Física* **29**, 645–648 (2007).

⁷ M. Abramowitz and I. A. Stegun, *Handbook of Mathematical Functions with Formulas, Graphs, and Mathematical Tables*, 9th ed. (Dover, New York, 1972), pp. 567–581.

⁸ A. Čēbers, “Dynamics of a chain of magnetic particles connected with elastic linkers,” *J. Phys.: Condens. Matter* **15**, S1335–S1344 (2003).